Determining and Accounting for a Parachute Virtual Mass

T. Yavuz*
Karadeniz Technical University, Trabzon, Turkey

The concept of virtual mass is described, and experiments are outlined in which virtual mass and virtual inertia components for a parachute canopy were determined. Results show that these components depend on the canopy shape and its attitude relative to the airflow; they also depend on the dimensionless acceleration, or acceleration number, of the parachute. Except at high values of acceleration number, these virtual inertia terms are of greater magnitude than corresponding values determined by potential flow methods, and this is characteristic of unsteady bluff-body flows. Their significance is indicated in dynamic behavior prediction for the descending fully deployed parachute canopy.

Nomenclature

A	= surface area of canopy
a_{ij}	= virtual mass components (Fig. 1)
C_D	= drag force coefficient $(= d/\frac{1}{2}\rho_f A V^2)$
C_R	= total force coefficient $(= z/\frac{1}{2}\rho_f A V^2)$
D	= drag force
D_0	= nominal diameter
I	= moment of inertia of body (subscripts denote relevant axes)
I_f	= reference moment of inertia of fluid displayed by body $(= 1/16\pi D^2 \forall)$
k_{ij}	= virtual mass coefficients (Fig. 1)
ℓ_D	= arm length (for cruciform canopy)
$M(L,M,N)$	= external moments about (x,y,z) axes
m	= body mass
$w(p,q,r)$	= angular velocity components about (x,y,z) axes
R	= total hydrodynamic force
(u,v,w)	= linear velocity components along (x,y,z) axes
V	= resultant velocity
$\dot{V}$	= acceleration
$F(X,Y,Z)$	= external forces along (x,y,z) axes
δ	= acceleration modulus $(= \dot{V}D_0/V^2)$
ρ_f	= fluid density
τ	= torsion
ω	= arm width (for cruciform canopy)
Ω	= angular velocity
$\dot{\Omega}$	= angular acceleration
$\forall$	= reference volume of fluid displaced by body $(= \frac{1}{2}\pi D_0^3)$

Introduction

WHEN parachutes with fully deployed canopies descend, their axes of symmetry may pitch about the vertical axis. Thus, angular accelerations in pitch occur, and these in turn lead to linear accelerations along the axis of symmetry and also at right angles to it. In determining the response of the parachute and store to disturbances in pitch, it is necessary to consider not only the inertias of the parachute but also those of the surrounding air. The work done by applied forces or moments causes an increase in kinetic energy of the parachute system comprising canopy and store and also of the surrounding air. Such a state of affairs occurs when work is done on any body immersed in a fluid. However, if the body density is large compared with that of the fluid, the increase in kinetic energy of the latter is negligible compared with the former. In classical hydrodynamic theory developed by Lamb[1] and others, the total kinetic energy of the fluid in a given direction is written in terms of that of the body, $\frac{1}{2}mV^2$, as $\frac{1}{2}a_{ii}V^2$, where a_{ii} is a virtual mass component, calculable if the flow of the fluid is considered to be potential. The virtual or apparent mass is a tensor quantity, varying in magnitude as the direction of body motion changes. The term can also be taken to include virtual moment of inertia components, defined for rotational motion in a similar manner to virtual mass coefficients in linear motion. Virtual mass components can be expressed in coefficient form when divided by an appropriate mass, generally taken to be equal to that of the fluid displaced or that mass displaced by some volume representative of the body. In the same way, virtual moment of inertia coefficients are formed by division of components by a representative moment of inertia. Virtual mass and moment of inertia coefficients evaluated by potential flow methods are constants for a given body shape and attitude.

The significance of these virtual inertia terms in the evaluation of parachute performance has long been appreciated and is commonly allowed for in dynamic stability analysis through the introduction of appropriate virtual mass and virtual moment of inertia coefficients. Such values have been obtained, notably by Ibrahim [2] by considering potential fluid flow about idealized parachute canopy shapes. In the present study, however, we have determined these coefficients experimentally. We show that they depend on parameters other than those considered in potential flow analysis and that their numerical values can greatly exceed potential flow determinations. In predicting response of the parachute system to pitch, it is therefore important to use experimentally obtained values of apparent mass and apparent moment of inertia coefficients.

Equations of Motion

For more than 65 years (Relf and Jones,[3] Frazer and Simmons,[4] Iversen and Balents,[5] and Keulagen and Carpenter[6]), there has been experimental evidence that, although potential flow methods yield virtual mass and moment of inertia coefficients that are acceptable for streamlined bodies, serious discrepancies arise when the bodies are bluff. For high drag forces to result from flow separation, it is essential for a parachute canopy to be unstreamlined; thus, it is unlikely that potential flow evaluations, which imply unseparated flows, will yield results that accord with experiment. Thus, we undertook a series of one- and two-dimensional experiments.

Received Jan. 29, 1988; revision received June 17, 1988.

*Faculty of Engineering.

If a parachute canopy of mass m is accelerated through a fluid with an acceleration $\dot{w}$ in the direction 0-z of its axis of symmetry, the force Z required to sustain that acceleration can be written as

$$Z=(m+a_{33})\dot{w} \tag{1}$$

From this expression, a_{33} and hence the virtual mass coefficient k_{33} can be evaluated:

$$k_{33}=a_{33}/\rho_f \forall \tag{2}$$

where ρ_f is the density of the fluid, and $\forall$ is the representative displaced volume, taken to be that of a hemisphere having a diameter D_0 equal to the nominal diameter of the canopy, i.e.,

$$\forall=(1/12)\pi D_0^3 \tag{3}$$

In exactly the same way, the force X required to accelerate the canopy perpendicular to its axis of symmetry in the direction 0-x is written as

$$X=(m+a_{11})\dot{u} \tag{4}$$

from which expression the virtual mass coefficient k_{11} is evaluated, i.e.,

$$k_{11}=a_{11}/\rho_f \forall \tag{5}$$

When the canopy executes angular accelerations about an axis 0-y through the axis of symmetry and perpendicular to the 0-x and 0-z axes, the torque L is related to angular acceleration $\dot{p}$ by

$$L=(I_{yy}+a_{55})\dot{p} \tag{6}$$

where I_{yy} is the moment of inertia of the canopy about the axis 0-y. The virtual moment of inertia coefficient k_{55} is then written as

$$k_{55}=a_{55}/I_f \tag{7}$$

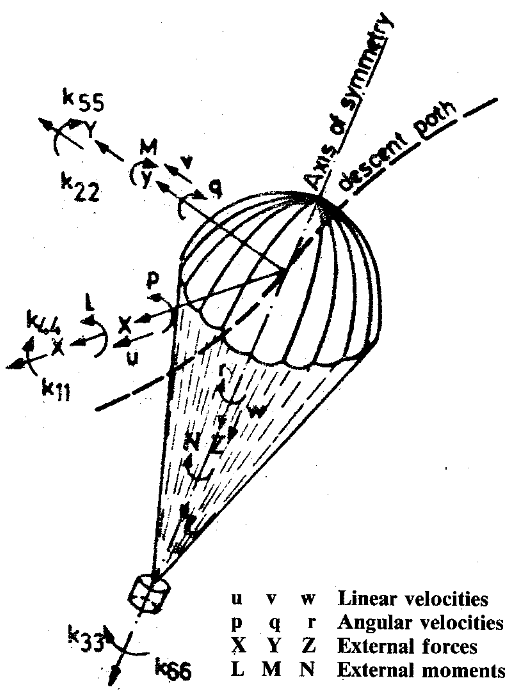

Fig. 1 Definition of terms in the equations of motion for the parachute.

where I_f is the representative moment of inertia of the displaced fluid, that is, the moment of inertia about an appropriate axis of the fluid displaced by a hemisphere of diameter D_0. For present purposes of evaluation, the appropriate axis is chosen to pass through the center of volume of the hemisphere. Then,

$$I_f=(1/16)D_0^2\rho_f \forall \tag{8}$$

where $\forall$ is defined in Eq. (3).

For a canopy that can be considered to be a body of revolution about the axis 0-z and that is rigidly attached to its store, as shown in Fig. 1, the appropriate equations of motion, which were derived by Cockrell and Doherr,[7] are

$$X=(m+a_{11})(\dot{u}-rv)+(m+a_{33})qw$$
$$+(mz_s+a_{15})(\dot{q}+rp) \tag{9a}$$
$$Y=(m+a_{11})(\dot{v}+ur)-(m+a_{33})pw$$
$$-(mz_s+a_{15})(\dot{p}-rq) \tag{9b}$$
$$Z=(m+a_{33})\dot{w}-(m+a_{11})(qu-pv)$$
$$-(mz_s+a_{15})(p^2+q^2) \tag{9c}$$
$$L=(I_{XX}+a_{55})\dot{p}-(mz_s+a_{15})(\dot{v}-pw+ru)$$
$$+(I_{ZZ}-I_{XX}-a_{55})qr+(a_{33}-a_{11})vw \tag{9d}$$
$$M=(I_{XX}+a_{55})\dot{q}+(mz_s+a_{15})(\dot{u}+qw+rv)$$
$$+(I_{XX}-I_{ZZ}+a_{55})pr-(a_{33}-a_{11})uw \tag{9e}$$
$$N=I_{ZZ}\dot{r} \tag{9f}$$

where (X,Y,Z) and $(L,M,N,)$ are the external forces and the external moments acting, respectively, along or about the x,y,z axes; (u,v,w) are the respective linear velocity components; and (p,q,r) are the respective angular velocity components. The mass of the system is denoted by m, and z_s is the distance measured along the z axis from the origin to the mass center. The symbols I_{XX} and I_{ZZ} are the moments of inertia of the canopy-store system measured about the x and z axes, respectively.

These equations for axisymmetric parachute contain four independent virtual mass or moment of inertia components:

$a_{11}=a_{22}$:	virtual mass component in direction 0-x or 0-y
a_{33}:	virtual mass component in direction 0-z
$a_{44}=a_{55}$:	virtual moment of inertia component about the axis 0-x or 0-y
$a_{15}=-a_{24}$:	virtual mass or moment of inertia component coupling motion along the axis 0-x to motion about axis 0-y or motion along the axis 0-y to motion about the axis 0-x

The derivation of Eqs. (9) from Kirchhof's equations assumes that a potential fluid surrounds the descending parachute, for the virtual mass coefficients in the equation are assumed to be invariant with time. To satisfy the relationships, the authors conducted a series of experiments from which the virtual mass coefficients k_{11}, k_{33}, and k_{55} were determined, using Eqs. (2), (5), and (7), for parachute canopies of differing shapes. Yavuz[8] shows that, if the coordinate system origin is at the canopy center of pressure, then $a_{15}=0$. Because the location of this center of pressure is neither fixed nor precisely known, the chosen origin was at the center of volume of a hemispherically shaped canopy, where a_{15} will be nonzero. However, in the course of these experiments, the authors were satisfied that it differed from zero by less than the experimental uncertainty of the measurements that were being made.

Experimenal Methods

Following experiments in which both Relf and Jones[3] and Frazer and Simmons[4] accelerated bluff bodies through large tanks of otherwise still water, the virtual masses of parachute canopies was determined by towing underwater scale models in the large ship tank at the College of Higher Education, Southampton, UK. The tank is 61 m long, 3.7 m wide, and 1.8 m deep. An associated towing carriage travels for most of the tank length over the water surface at a constant velocity that can be adjusted up to about 5 m/s, accelerating and decelerating rapidly at each end of the tank. Water was chosen as a suitable medium for these experiments because Eqs. (1-7) indicate that, for potential flow virtual mass and moment of inertia coefficients, the forces and moments generated by accelerating bodies underwater are three orders of magnitude greater than those when the same bodies accelerate at the same rate through air. Underwater there was no discernible difference to the shape of the parachute canopy from that observed when it flew through air. Model canopies used have a flight diameter of 0.30 m, and Reynolds numbers achieved were about one-fourth those for full-scale canopies descending in air. Jorgensen[9] has shown that this difference in Reynolds number is of little significance for a parachute canopy.

Following Iversen and Balent,[5] a dimensionless linear acceleration number δ was defined in terms of the canopy nominal diameter D_0:

$$\delta = \dot{V} D_0 / V^2 \tag{10}$$

where $\dot{V} = \dot{V}_X$ for x-directed motion and $\dot{V}_Z$ for z-directed motion (Fig. 1). Since there was only a limited facility for the ship tank towing carriage to impart to suspended models the necessary accelerations and decelerations, a piston and crank mechanism shown in Figs. 2a and 2b was specially devised to meet this end. Figure 3 shows this mechanism slung beneath the towing carriage, with the parachute canopy models mounted from it on strain-gage string supports.

The piston and crank mechanism is carried on an inner circular ring that is capable of rotation relative to an outer ring. This, in turn, is rigidly attached to the towing carriage. By rotating the inner ring, the track along which piston A (Fig. 2a) moves is aligned either parallel or perpendicular to the longitudinal axis of the ship tank, or, if desired, it can be set at known intermediate positions. While being towed through the water by the motion of the carriage, the parachute canopy can thus be oscillated harmonically at a low frequency along any line in the plane parallel to the tank bed. Since the piston linear velocity and linear acceleration along this line are known functions of angular velocity and displacement of the crank, the acceleration number is calculable. The corresponding virtual mass coefficients k_{33} or k_{11} are determined from Eqs. (3) and (5) from knowledge of the appropriate internal forces developed on the strain-gage string, as shown in Fig. 4.

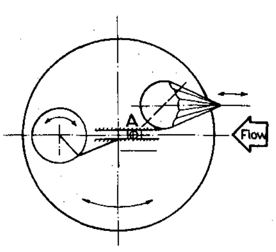

a) Mechanism imparting linear acceleration

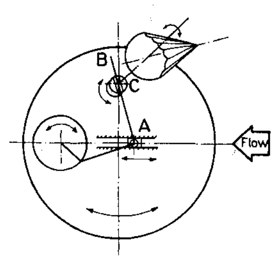

b) Mechanism imparting angular acceleration

Fig. 2 Piston and crank mechanisms.

To determine the virtual moment of inertia coefficient k_{55}, the apparatus used in Fig. 2b was used instead of that in Fig. 2a. A bar AB is pin-joined to the piston at A and is free to move through a swivel block at C, to which the canopy sting is now attached. By this means angular motion, without translation, can be imparted to the parachute canopies. Again, the angular velocity and the angular acceleration of the swivel block and hence the parachute canopy are known functions of both the angular velocity and the displacement of the crank. The torque in the supporting sting is given from the appropriate strain-gage bridge output.

Outputs from all of the strain-gage bridges, along with the signals that represent the displacement of the towing carriage and the angular displacement of the crank, were recorded as analog signals by a multichannel chart recorder. From these records were determined the three required virtual mass and moment of inertia components: a_{11}, a_{33}, and a_{55}.

Potential Flow and Other Experimental Solutions

To obtain potential flow solutions for these three virtual mass components, Tory and Ayres[10] represented the parachute canopy, together with the virtually stagnant air within it, as though it were a planetary ellipsoid, circular in plan when viewed along the parachute axis of symmetry and elliptical, with a ratio of minor to major axes of 1:2, when viewed from the side. Lamb[1] had derived expressions for the virtual masses and moment of inertias of the flow around ellipsoids of revolution, but these expressions did not include the mass or the requisite moments of inertia of the fluid contained within these ellipsoids. Tory and Ayres therefore added these to Lamb's evaluations, giving rise to the concept of included mass as an addition to the virtual (or apparent) mass that Lamb had calculated.

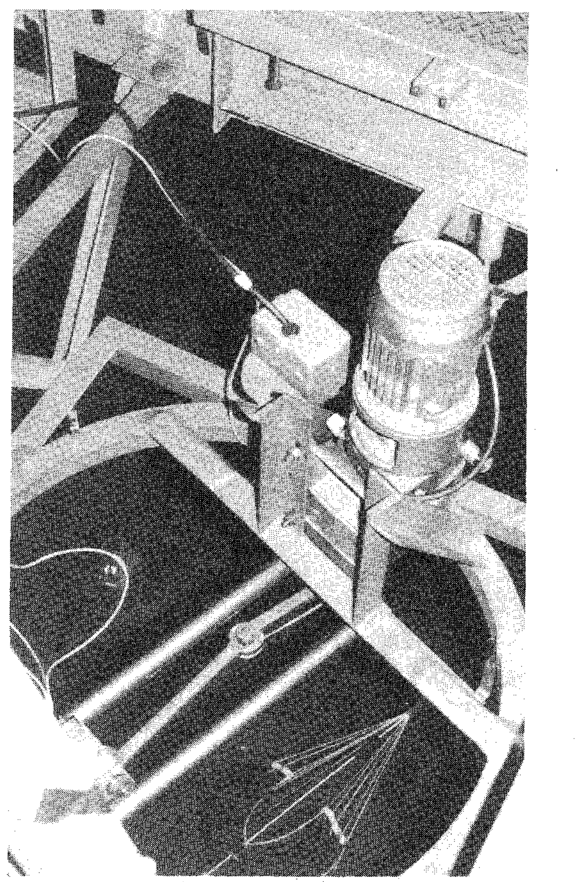

Fig. 3 Photograph of piston and crank mechanism slung from the towing carriage.

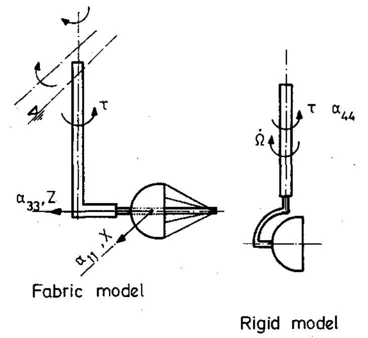

Fig. 4 Determination of forces and moments acting on the model parachute canopies.

Writing the virtual mass and inertia component of the fluid a_{ii} in terms of the mass m_e or the moment of inertia I_e, measured about the major axis of the planetary ellipsoid, then

$$a_{11} = (1 + k_{11}) m_e \tag{11a}$$

$$a_{33} = (1 + k_{33}) m_e \tag{11b}$$

$$a_{55} = (1 + k_{55}) I_e \tag{11c}$$

where k_{ii} are Lamb's determinations, and the mass and moment of inertia of the fluid within the ellipsoid have also been included.

Appropriate potential flow values of the virtual mass coefficients are

$(1 + k_{11}) = 1.31$ in direction 0-x (12a)

$(1 + k_{33}) = 2.12$ in direction 0-z (12b)

$(1 + k_{55}) = 1.34$ about axis 0-y (12c)

Since the volume of the planetary ellipsoid representative of the stagnant air is equal to that of a hemisphere whose diameter equals twice the major axis of the ellipsoid, the first two coefficients are already appropriately scaled in terms of the representative displaced volume ∀ in Eq. (2). However, the moment of inertia of a planetary ellipsoid about its major axis is one-fifth that of a hemisphere about its center of volume, determined in Eq. (8). Thus, with the appropriate representative volumes and moments of inertia, Lamb's theoretical determinations as modified by Tory and Ayres[10] become

$$k_{11} = 1.31 \tag{13a}$$

$$k_{33} = 2.12 \tag{13b}$$

$$k_{55} = 0.27 \tag{13c}$$

In this model of apparent moment of inertia, the included mass of air is implicitly assumed to be in solid-body rotation; thus, its theoretical evaluation is the least plausible of the three. By considering the parachute canopy to be represented by a shallow horizontal cup, Ibrahim[2] derived k_{33} in potential flow equal to 1.6. Ibrahim[11] also conducted experiments to obtain the virtual moment of inertia of parachutes. He believed that his technique, which produced results for the virtual mass of disks, cubes, and spheres which exceeded potential flow evaluations, but by less than 20%, produced results for virtual moment of inertia which would approximate closely the potential flow evaluations. For imporous hemispherical canopies rotating about an axis through the center of volume of the included mass, he obtained approximate experimental

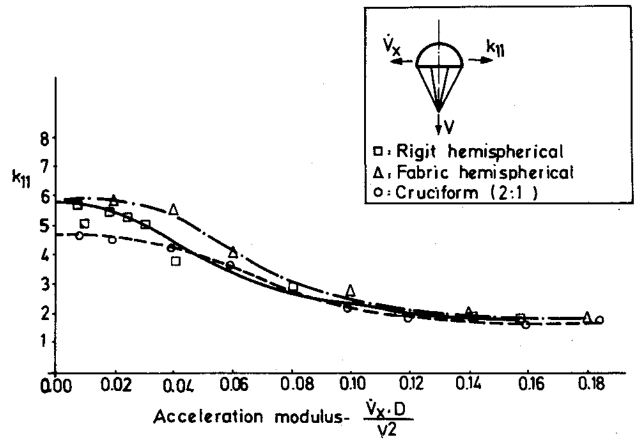

Fig. 5 Variation of virtual mass coefficient k_{11} for hemispherical-cruciform (2:1) canopies with linear acceleration number.

values of 0.0037 $\rho_f \pi D_0^5$; hence, with the representative moment of inertia of Eq. (8), Ibrahim's experimental value for k_{55} would equal 0.70. This differs significantly from the values of 0.27 in Eqs. (13). In Ibrahim's experiments he showed k_{55} to be strongly dependent on canopy porosity. In their paper on parachute dynamic stability, White and Wolf[12] used these latter values for k_{33} and k_{55}. However, they assumed k_{33} to be independent of direction, thus taking k_{11} also to equal 1.6.

Experimental Results and Discussion

The equation of Morrison et al.[13] for fluid resistance F on a body of mass m that moves unsteadily can be written as

$$F = D + (m + a)\dot{V} \tag{14}$$

where D is the steady-state drag, a is the virtual mass of the body, and $\dot{V}$ is its acceleration. Written in terms of a generalized force in unsteady motion R_{ij} and a steady-state force D_{ij},

$$R_{ij} = D_{ij} + (m + a_{ij})\dot{V}_{ij} \tag{15}$$

This can be nondimensionalized to

$$C_{R_{ij}} = C_{D_{ij}} + (m + a_{ij})(2\dot{V}_{ij}/V^2 \rho_f A) \tag{16}$$

which, if the mass of the body is negligible compared with its virtual mass, gives for the virtual mass coefficient k_{ii} in terms of the acceleration number δ

$$k_{ii} = c\delta (C_{R_{ii}} - C_{D_{ii}}) \tag{17}$$

where the magnitude of the constant c depends on the definitions for the representative area adopted in the expressions for C_D and C_R, and the represenative volume adopted in the expression for acceleration number δ.

In the same way, if the moment of inertia of the body is negligible compared with the representative moment of inertia of the fluid I_f, the virtual moment of inertia coefficient can be expressed in terms of the torque developed, as τ:

$$k_{ii} = \tau / \dot{\Omega} I_f \tag{18}$$

In the ship tank experiments, Eqs. (17) and (18) were adopted to establish values of the coefficients k_{11}, k_{33}, and k_{55}. If the period of the oscillatory motion were short enough for it to affect the flow around the immersed body, Keulegan and Carpenter[6] show that the required coefficients are functions of this period. However, in the experimental program adopted, this period was not short. Independent experiments were conducted to ensure that it did not affect the values of the parameters which were obtained. In these, the acceleration and the deceleration of the towing carriage at the extremities of its travel rather than the piston-crank mechanism were used to impart the unsteady motion to the parachute canopies. Yavuz[8] shows that the results obtained from these experiments were indistinguishable from those with the long-period motion imparted by the piston-crank mechanism.

In Figs. 5 and 6, values of the virtual mass coefficient at right angles to the axis of symmetry k_{11} are shown varying with acceleration number δ at a constant angle of attack and varying with angle of attack at a constant acceleration number. These results were obtained for a flexible but imporous hemispherical and cruciform parachute canopy models. They show that, at low values of acceleration number, k_{11} is several times larger than the potential flow evaluation of about 1.3. As acceleration number increases, however, k_{11} decreases, possibly tending asymptotically to the potential flow value. If high acceleration number is considered as representative of a high acceleration of a bluff body that is accompanied by a low velocity, it would be a characteristic of the flow around that body when the latter began moving from rest. Under these conditions the vorticity in the flow at the body boundary would be small, resulting in negligible flow separation, and the resulting flowfield might well be considered to be potential.

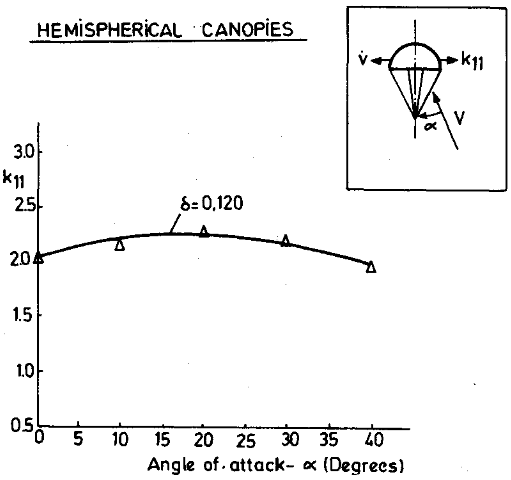

Fig. 6 Variation of virtual mass coefficient k_π for hemispherical canopy with angle of attack.

Measurements made of k_{11} as the angle of attack is varied show this virtual mass coefficient to be virtually independent of angle of attack and hence of canopy shape, since, as the angle of attack changes, the shape of the canopy presented to the flow alters significantly. The nominal canopy diameter D_0 in Eqs. (3), (8), and (10), respectively, for the representative volume, representative moment of inertia, and acceleration number was taken to be the projected diameter of the hemispherical canopy at zero angle of attack.

In Figs. 7 and 8, values of the virtual mass coefficient in the axis of symmetry direction k_{33} are shown as functions of both acceleration number and angle of attack, obtained for the flexible but imporous hemispherical canopy and also for flexible and imporous flat cruciform canopies of various arm ratios. For these latter canopies, the total distance from the canopy hem, through the canopy apex, and back to the hem is designated as ℓ_p, and the arm width is designated as ω. Then, the nominal area S_0 and nominal diameter D_0 for the canopies are given by

$$S_0 = \omega(2\ell_p - \omega) \tag{19}$$

$$D_0 = (4S_0/\pi)^{1/2} \tag{20}$$

Like those for k_{11} the calculations show k_{33} to be strongly dependent on acceleration number, several times larger than the potential flow evaluation of about 2.0 when the acceleration number is small. Again, there is a tendency for the k_{33} characteristics to approach the potential flow value of about 2.0 when acceleration numbers are high. Results are much more dependent on canopy shape than are those for k_{11}. This fact is confirmed by large changes in k_{33} caused by the effective change in shape of the canopy which occurs because of varying angle of attack. It is also evident from the significant differences in k_{33} values at negative acceleration numbers from those when the acceleration numbers are D_0 positive, for a decelerating canopy is of a different shape from an accelerating one.

Since flexible model canopies were found to collapse at the relatively high angular accelerations imparted by the modified piston and crank mechanism of Fig. 3b, results shown in Fig. 9 for the virtual moment of inertia coefficient k_{55} were obtained with a rigid imporous hemispherical canopy model having a projected diameter D_0 of 0.30 m. Motion was imparted by the piston-crank mechanism to the canopy when the towing carriage was at rest.

As in all of the other experiments described, the data extracted from the experiments were obtained at the two extreme positions of the piston-crank mechanism, when the velocity imparted to the immersed model was zero but its acceleration was a maximum. In the virtual mass coefficient experiments,

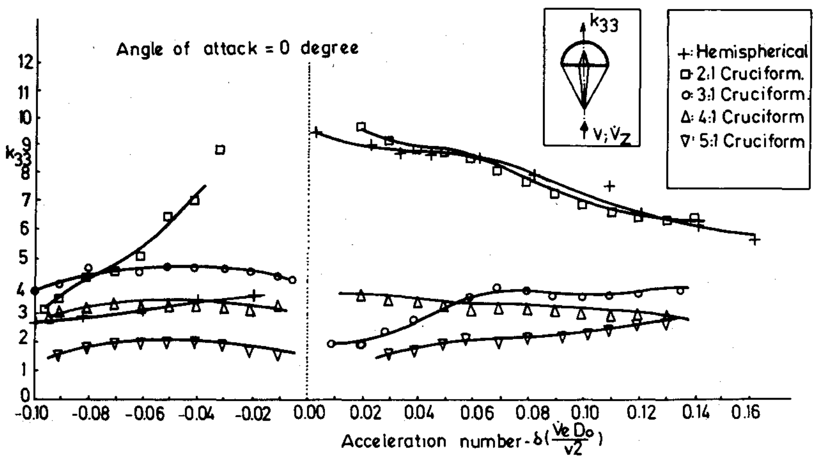

Fig. 7 Variation of virtual mass coefficient k_{33} for hemispherical and cruciform canopies with linear acceleration number.

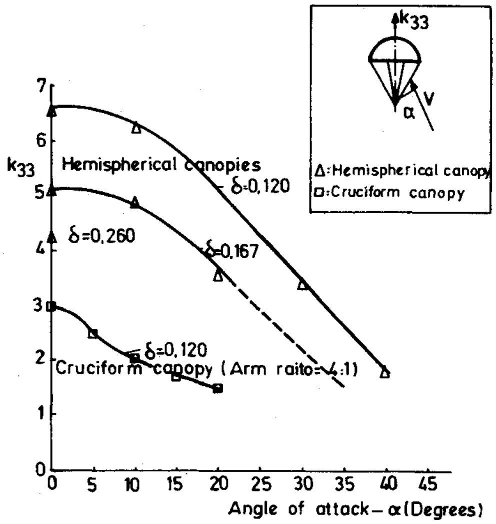

Fig. 8 Variation of virtual mass coefficient k_{33} for hemispherical and cruciform canopies with angle of attack.

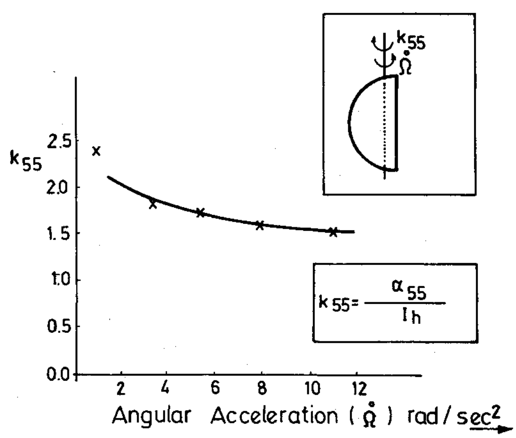

Fig. 9 Variation of virtual moment of inertia coefficient k_{55} for rigid hemispherical canopy with angular acceleration.

there was towing carriage motion simultaneous with that of the piston crank mechanism; thus, even at instants when the latter imparted no velocity to the immersed models, the flow around these models possessed relative velocity, and values of this velocity were used to determine relevant acceleration numbers. However, all of the angular motion data presented in Fig. 9 represent conditions when there was no angular velocity of the model. Thus, if plotted against angular acceleration number, defined as $\dot{\Omega}/\Omega$, they would all occur at very high values of the latter. It is suggested that there is a spread in values of k_{55} which has been obtained because the angular velocity of the fluid field is not zero at the instant at which the angular velocity of the immersed body that promotes it is zero. Values of k_{55} shown in Fig. 9 do not vary appreciably with angular acceleration and bear some comparison with the experimental value of 0.7, which Ibrahim[11] independently obtained.

Conclusions

Virtual inertia terms, the magnitudes of which have a significant effect on predictions of parachute dynamic performance, have been shown by experiment to possess values that may greatly exceed those estimated by potential methods. These virtual inertia terms generally vary with acceleration number, tending to potential flow evaluations as the acceleration number increases. The virtual mass coefficient in the direction of the canopy axis of symmetry varies significantly with canopy shape, but the coefficient at right angles to the axis of symmetry is much less dependent on shape. There is independent evidence that both coefficients are functions of canopy porosity. Values of about 1.5 obtained for the virtual moment of inertia coefficient k_{55} bear some comparison with other values obtained by Ibrahim, who used an independent technique.

Since these measured virtual inertia terms do significantly affect predictions of pitching oscillation damping rate, it is clear that contemporary mathematical models for parachute descent behavior, which rely on potential flow evaluations, can no longer be considered satisfactory. Not only do they underestimate the values that have been determined experimentally, but they also do not account for the significant variation of coefficients with both acceleration number and angle of attack which has been observed in the experimental program described. Further experimental data relevant to other parachute canopy shapes are clearly necessary.

References

[1]Lamb, H., *Hydrodynamics*, 6th ed., Cambridge Univ. Press, Cambridge, UK, 1932.

[2]Ibrahim, S. K., "Apparent Added Mass and Moment of Inertia of Cup-Shaped Bodies in Unsteady Incompressible Flow," Ph.D. Thesis, Univ. of Minnesota, May 1965.

[3]Relf, E. F. and Jones, M. A., "Measurement of the Effect of Accelerations on the Longitudinal and Lateral Motion of an Airship Model," UK Advisory Committee for Aeronautics, R&M 613, 1981.

[4]Frazer, R. A. and Simmons, L. F. G., "The Dependence of the Resistance of Bodies Upon Acceleration, as Determined by Chronograph Analysis," UK Advisory Committee for Aeronautics, R&M 590, 1919.

[5]Iversen, H. W. and Balent, R., "A Correlating Modulus for Fluid Resistance in Accelerated Motion," *Journal of Applied Physics,* Vol. 22, No. 3, March 1951.

[6]Keulegan, G. H. and Carpenter, L. H., "Forces on Cylinders and Plates in an Oscillating Fluid," *Journal of Research of the National Bureau of Standards,* Vol. 60, No. 5, May 1958, Paper 2857.

[7]Cockrell, D. J. aand Doherr, K. F., "Preliminary Consideration of Parameter Identification Analysis from Parachute Aerodynamics Flight Test Data," AIAA Paper 81-1940, Oct. 1981.

[8]Yavuz, T., "Aerodynamics of Parachutes and Like Bodies in Unsteady Motion," Ph.D. Thesis, Univ. of Leicester, Leicester, UK, 1982.

[9]Jorgensen, D. S., "Cruciform Parachute Aerodynamics," Ph.D. Thesis, Univ. of Leicester, Leicester, UK, 1982.

[10]Tory, C. and Ayres, R., "Computer Model of a Fully Deployed Parachute," *Journal of Aircraft,* Vol. 14, July 1977.

[11]Ibrahim, S. K., "Experimental Determination of the Apparent Moment of Inertia of Parachutes," Air Force Flight Dynamics Lab., TDR-64-153, Wright-Patterson AFB, April 1965.

[12]White, F. M. and Wolf, D. F., "A Theory of Three-Dimensional Parachute Dynamic Stability," *Journal of Aircraft*, Vol. 5, Jan. 1968.

[13]Morrison, J. R., O'Brien, M. P., Johnson, J. W., and Shaaf, S. A., "The Force Exerted by Surface Waves on Piles," *Petroleum Transactions,* Vol. 189, 1950.